doi:10.1038/nature09565

		Page
1.	**Mathematical Modelling**	**2**
1.1	Models of Input Promoters	**2**
	Supplementary Figure 1: Binding states of the P_{BAD}, P_{Tet}, and P_{Las} promoters	
	Supplementary Figure 2: The transfer function of the P_{Las} promoter	
	Supplementary Table 1: Parameters for the P_{BAD}, P_{Tet}, and P_{Las} promoters	
1.2	Model of Tandem Promoters	**5**
	Supplementary Figure 3: Interference in tandem promoters	
1.3	NOT Gate Model	**6**
	Supplementary Figure 4: Binding states of the P_{CI} promoter	
	Supplementary Figure 5: The transfer function of the P_{CI} promoter	
	Supplementary Table 2: NOT gate parameters	
2.	**Flow Cytometry Data**	**8**
	Supplementary Figure 6: Flow cytometry data for all possible two-input logic gate	
	Supplementary Figure 7: Dynamic range for various Boolean logic gates constructed	
3.	**Comparison of Liquid and Plate-based Cytometry Distributions**	**9**
	Supplementary Figure 8: Comparison of the distributions for the NOT A gate	
	Supplementary Figure 9: Population averaging effect	
4.	**Robustness in Plate Assay Conditions**	**10**
	Supplementary Figure 10: Distance, time interval, and density dependence	
	Supplementary Table 3: PDE model parameters	
	Supplementary Figure 11: XOR gate time delay dependence	
5.	**Liquid Culture Assay**	**13**
	Supplementary Figure 12: The XOR circuit as measured in liquid culture	
6.	**Strains, Plasmid Maps, and Plasmid Constructions**	**15**
	Supplementary Table 4: Bacterial strain list	
	Supplementary Table 5: List of plasmid parts and their sources	
7.	**Supplemental References**	**19**

1. Mathematical Modelling

1.1. Models of Input Promoters

The binding of ligands to transcription factors and transcription factors to DNA is modelled for three inducible promoters (Ara-inducible P_{BAD}, aTc-inducible P_{Tet}, and 3OC12-HSL inducible P_{Las}). The binding of a ligand to its transcription factor at equilibrium is

$$C = C_0 \frac{L^n}{K_d^n + L^n} \quad , \tag{1}$$

where C is the concentration of bound transcription factor, C_0 is the total concentration of transcription factors, L is the concentrations of ligands, K_d is the dissociation constant, and n is the cooperativity. By mass conservation, the concentration of free transcription factor C_F is

$$C_F = C_0 - C \quad . \tag{2}$$

The binding of transcription factors to their promoters are modelled according to the Shea-Ackers formulism[1-3]. The binding states for each promoter are shown in Supplementary Figure 1. The probability for each promoter being in open complex P is described by the following equations:

$$P_{BAD} = \frac{K_1 + K_2 C}{1 + K_1 + K_2 C + K_3 C_F} \quad , \tag{3}$$

$$P_{Tet} = \frac{K_1}{1 + K_1 + 2K_2 C_F + K_2^{\,2} C_F^{\,2}} \quad \text{and} \tag{4}$$

$$P_{Las} = \frac{K_1 + K_2 C}{1 + K_1 + K_2 C} \quad . \tag{5}$$

To parameterize Equations 3-5, the transfer functions of each promoter are determined by varying the concentration of inducer and measuring the expression of YFP (plasmids pOR10, pOR20, and pOR30). Parameters are fit to the normalized fluorescence data for each promoter (Supplementary Table 1). The plot of the model transfer function using these parameters for the P_{BAD} and P_{Tet} promoters are shown in Fig. 1c and in Supplementary Figure 2 for the P_{Las} promoter.

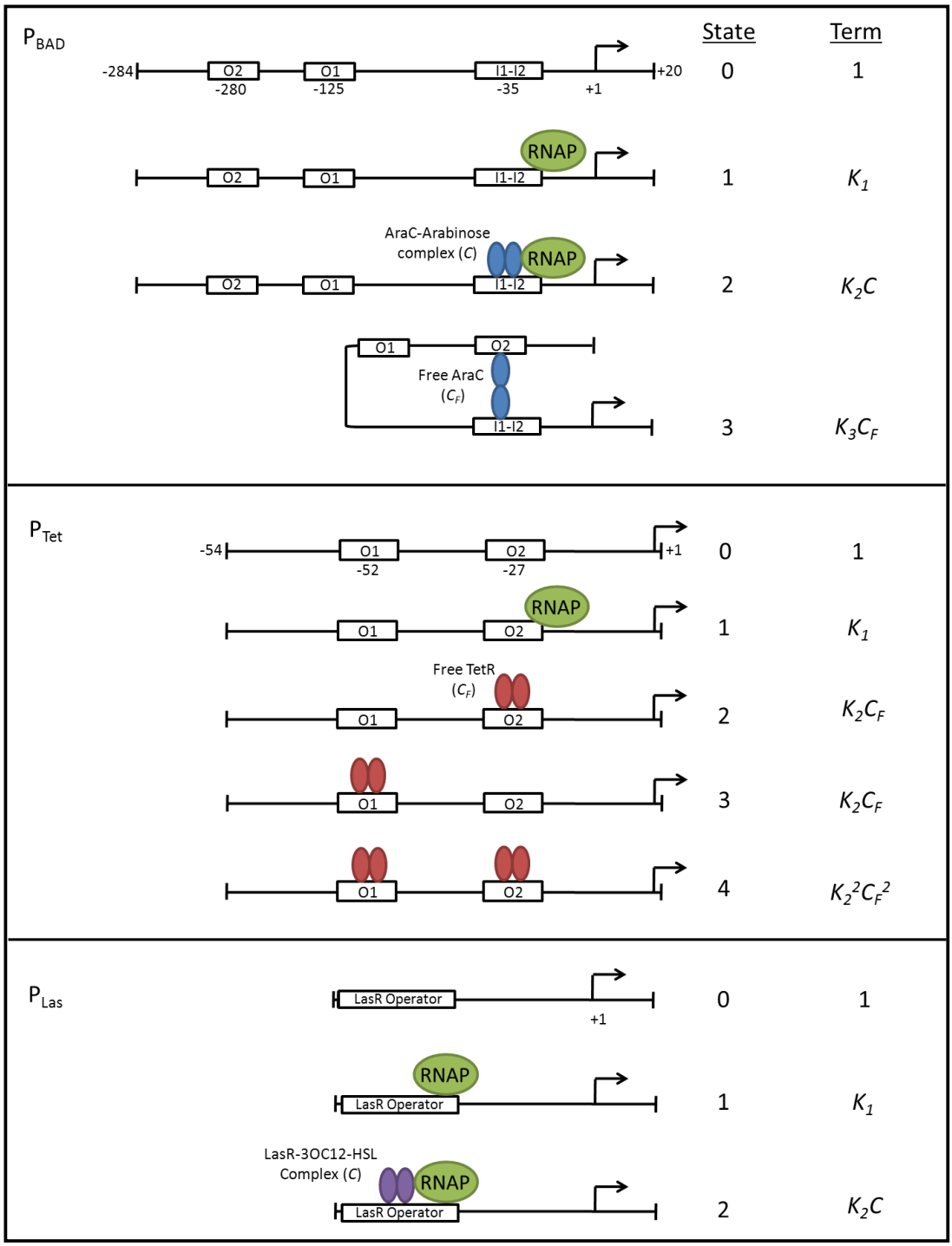

Supplementary Figure 1: The binding states of the P_{BAD}, P_{Tet}, and P_{Las} promoters used to generate Equations 3-5 are shown. The numbers correspond to the location of operator sites and promoter boundaries with respect to the +1 transcription start site. The terms of the partition function for each state are shown on the right. The concentration of RNAP is assumed to be constant and some potential states (not shown) are assumed to be infrequently occupied to reduce the number of parameters.

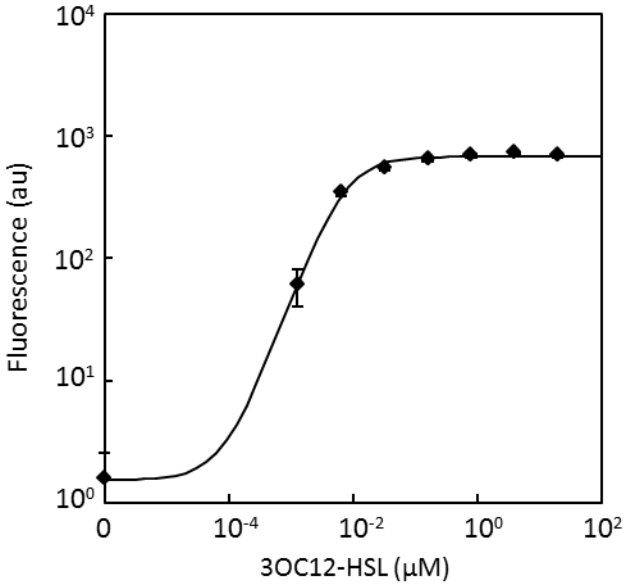

Supplementary Figure 2: The transfer function of the P_{Las} promoter. The fit to the model is shown as the solid line. Fluorescence values and their error bars are calculated as averages and one standard deviation from three experiments.

Supplementary Table 1: Parameters for the P_{BAD}, P_{Tet}, and P_{Las} promoters

Parameters	P_{BAD}	P_{Tet}	P_{Las}
K_d	0.09 mM	1.7 ng/mL	0.2 μM [a]
n	2.8	1.0	1.4
K_1	0.009	350 [a]	0.002
K_2C_0	37.5	160	100
K_3C_0	3.4		
gfp^{max} [b]	7650 au	3000 au	690 au

[a] Parameter was set according to the literature value[4,6].
[b] The fluorescence produced at maximum induction.

1.2. Model of Tandem Promoters

When two promoters control the transcription of a gene, the promoters can be additive or they could interfere with each other (either positively or negatively). In the additive case, the production of protein *X* is modelled as,

$$\frac{dX}{dt} = a_U b_U P_U + a_D b_D P_D - \gamma X \,, \tag{6}$$

where P_i is the probability of promoter *i* being in the open complex, a_i is the maximum transcription rate, b_i is protein production rate, and γ is the degradation rate. The subscripts U and D indicate the upstream and downstream promoter, respectively (Supplementary Figure 3). Considering the individually measured transfer functions, Equation 6 reduces to the following at steady-state,

$$X = \frac{a_U b_U}{\gamma} P_U + \frac{a_D b_D}{\gamma} P_D = X_U^{\max} P_U + X_D^{\max} P_D, \tag{7}$$

where $X_U^{\max}$ and $X_D^{\max}$ are the maximum concentrations of protein produced from each promoter independently at steady-state. Note that Equation 7 reflects a model of an OR gate, where the two one-dimensional transfer functions of the input promoters are used to generate the two-dimensional transfer function of the gate. This equation is used to generate the "predicted" transfer functions in Fig. 2a.

There are a number of ways that the two promoters could interfere with each other. If adding a downstream promoter impacts an upstream promoter – either by changing the transcription, mRNA degradation, or protein expression rates – then this effect can be included as a linear factor α_U (Supplementary Figure 3a). Similarly, if the upstream promoter impacts the parameters of the downstream promoter, then this can be included as a linear factor α_D. Together, this yields the modified transfer functions,

$$X = \alpha_U X_U^{\max} P_U + \alpha_D X_D^{\max} P_D \,. \tag{8}$$

To model the non-additive effect of combining two promoters, the two-dimensional transfer function of tandem promoters is fit to Equation 8 and α_U and α_D are treated as fit parameters. The values of the parameters that give the best fit quantify the degree to which there is interference between promoters. In most cases, the value of these parameters is ~1 for tandem promoters, indicating that they are behaving additively (Supplementary Figure 3c). Very high or low values of α indicate interference. For example, P_{BAD} exhibits significant interference when it is placed in the downstream position.

The simple factors in Equation 8 are sufficient to explain the interference that occurs between the P_{BAD} and P_{Tet} promoters. More complex interference could occur between promoters and this would require additional terms. For example, if the binding of a transcription factor to one promoter impacts the free energy of transcription factors binding to the second promoter, then this would not be captured in Equation 8. Similarly, if the activity of one promoter was impacted non-linearly by the activity of the second promoter, this would require more complex treatment.

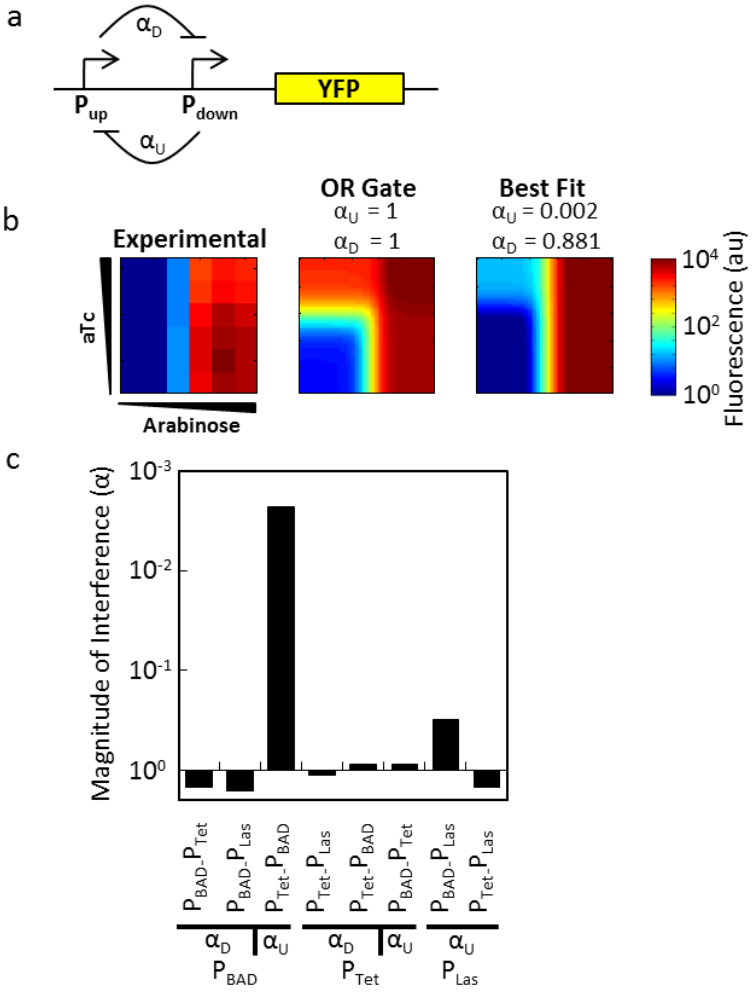

Supplementary Figure 3: An example of interference between tandem promoters is shown. a, The parameter α_D is the interference that an upstream promoter exerts on downstream promoters. The parameter α_U is the interference that a downstream promoter exerts on upstream promoters. **b,** The experimentally-obtained transfer function of the P_{Tet}-P_{BAD} tandem promoters is shown (plasmid pOR2010). If there was no interference, these tandem promoters should behave as an OR gate ($\alpha_U = \alpha_D = 1$). The transfer functions are shown with $\alpha_U = \alpha_D = 1$ set to one (middle) as well as with α_U and α_D values from a best fit (right). **c,** The interference factors are compared for all of the promoters used in this study. The tandem promoter pairs used to obtain the α_U and α_D values are shown.

1.3. NOT Gate Model

The repression of the P_{CI} promoter by CI is modelled using the Shea-Ackers formulism[1-3] with the promoter states shown in Supplementary Figure 4. The probability of the promoter forming an open complex is

$$P_R = \frac{K_1}{1 + K_1 + K_2 R + K_3 R + K_2 K_3 K_0 R^2} \quad , \qquad (9)$$

where R is the concentration of repressors and the binding constants are as described in Supplementary Figure 4. The objective of the model is to be able to predict how a NOR gate will behave when two input promoters are connected. As such, Equation 9 is parameterized as a NOT gate using the P_{Tet} promoter as an input. The output of P_{Tet}, as measured using YFP, is used as a surrogate for the repressor concentration in Equation 9. In this way, it can be predicted whether a particular promoter can be connected to the gate by measuring its transfer function using the same genetic background and reporter. This approach has been used previously to characterize an AND gate[5]. The experimental data for the transfer function of the NOT gate is shown in Supplementary Figure 5. Equation 9 is combined with Equations 3-5 to generate the "predicted" transfer functions of the NOR gate in Fig. 2b. For a particular gate, the transfer functions of the two input promoters are additively combined (Equation 7) and this is used as R in Equation 9.

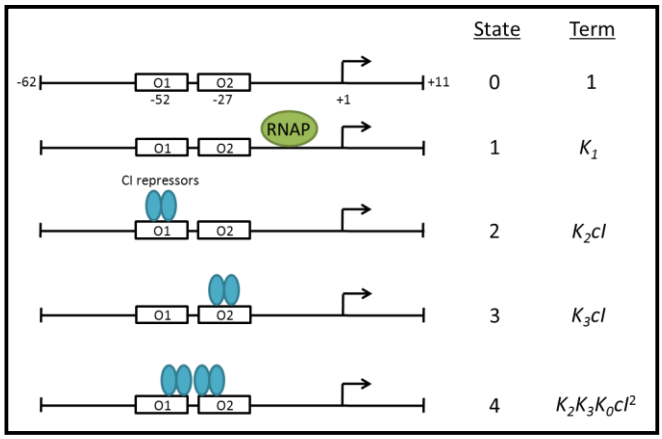

Supplementary Figure 4: Schematic diagram of the binding states used to model the P_{CI} promoter. The numbers correspond to the location of operator sites and promoter boundaries with respect to the +1 transcription start site. The partition function terms for each state are shown on the right. The concentration of RNAP is assumed to be constant.

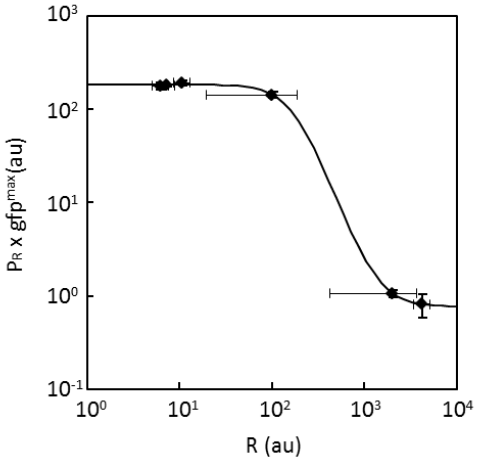

Supplementary Figure 5: The transfer function of the P_{CI} promoter. Each point represents a single concentration of aTc. The output of the P_{Tet} promoter (R) is measured using plasmid pOR1020 and the output of the NOT gate is measured in a separate experiment using plasmid pCI-YFP and pNOR1020. The concentrations of of aTc are (0, 0.025, 0.25, 2.5, 25, 250 ng/mL). The fit to Equation 9 is shown as the solid line. Fluorescence values and their error bars are calculated as averages and one standard deviation from three experiments.

Supplementary Table 2: NOT Gate Parameters

Parameters	
K_1	350 [a]
K_2	0.015 au^{-1}
K_3	0.5 au^{-1}
K_0	0.18
gfp^{max} [b]	181 au

[a] Parameter was estimated from the literature value [6].
[b] The fluorescence produced at maximum induction.

2. Flow Cytometry Data

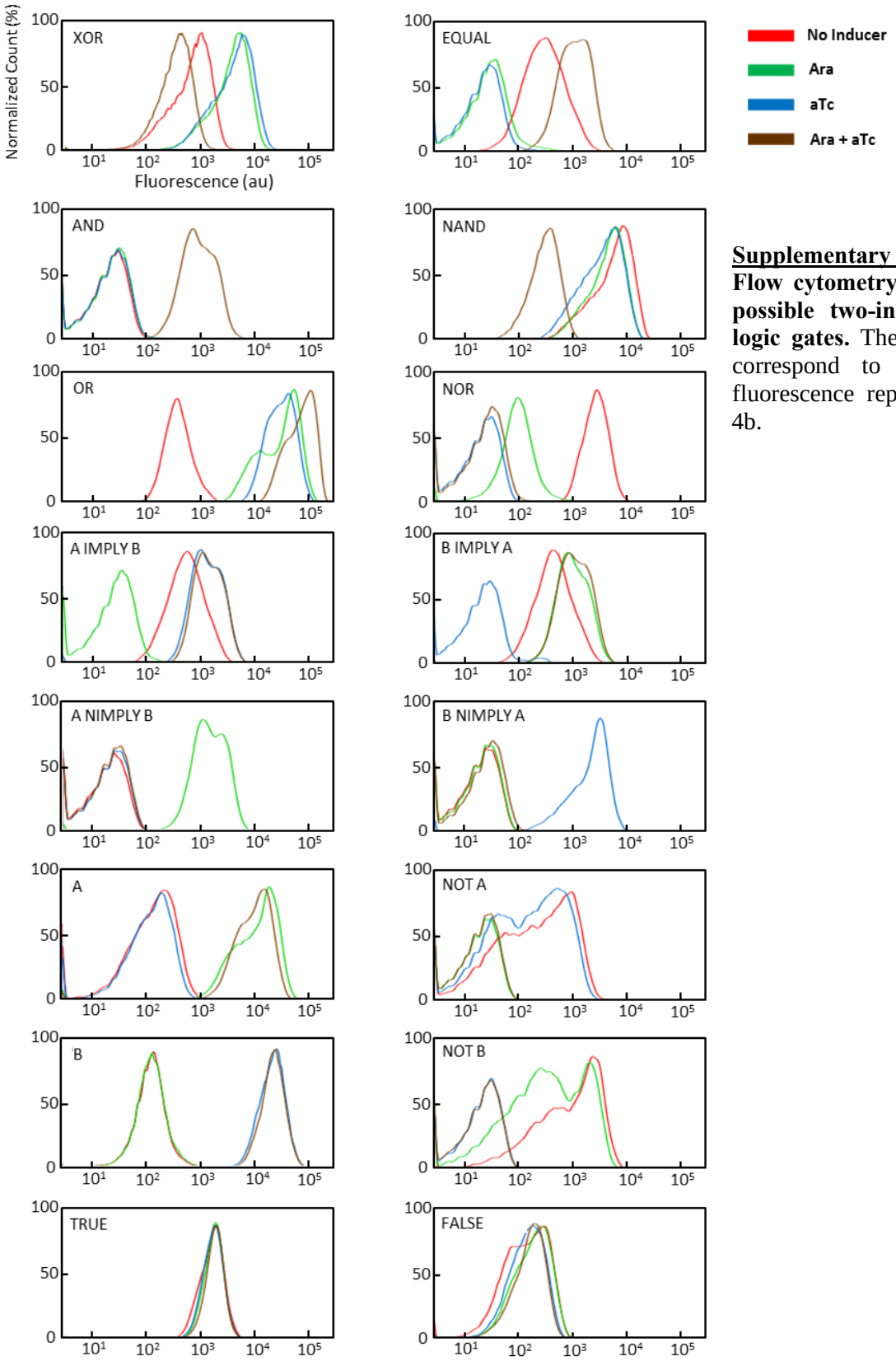

Supplementary Figure 6: Flow cytometry data for all possible two-input Boolean logic gates. The distributions correspond to the average fluorescence reported in Fig. 4b.

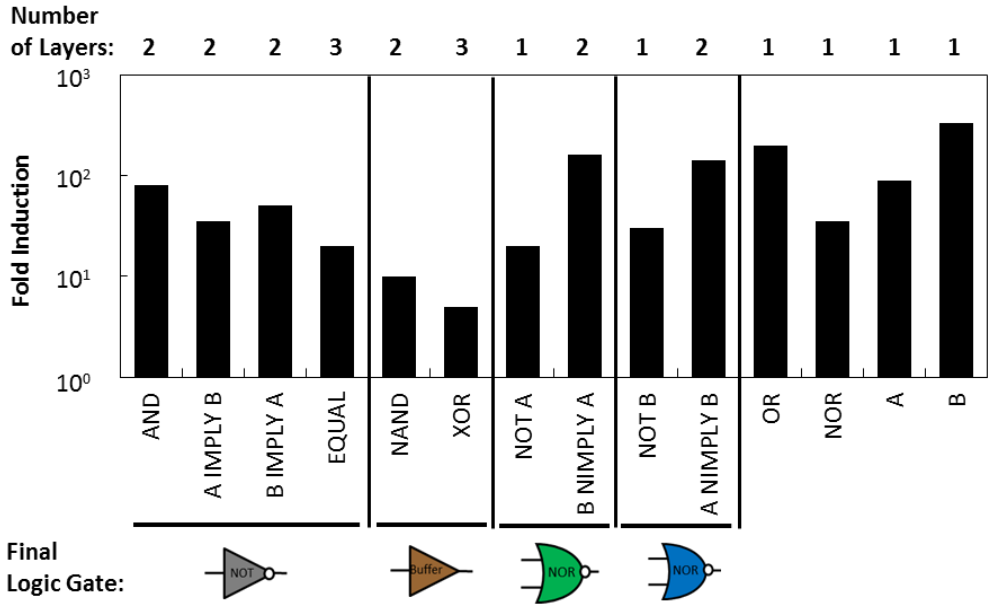

Supplementary Figure 7: The fold induction is shown for each circuit. Fold induction is defined as the ratio of the lowest ON state to the highest OFF state. The number of layers and the last gate is shown for each circuit.

3. Comparison of Liquid and Plate-based Cytometry Distributions

Some of the cytometry distributions in Supplementary Figure 6 show broad and/or bimodal distributions. We tested whether this variability is due to population heterogeneity within a colony grown on an agar plate. In Supplementary Figure 8, the population distributions of the NOT A gate are compared for liquid culture and plate assays. The distribution produced from a liquid culture shows a single peak, as is expected based on previous work[7,8]. It is interesting that the variability that occurs within a colony does not propagate to downstream layers for the more complex logic gates. The response of the population is averaged by the production of a quorum signal, which increases the robustness of the computation (Supplementary Figure 9).

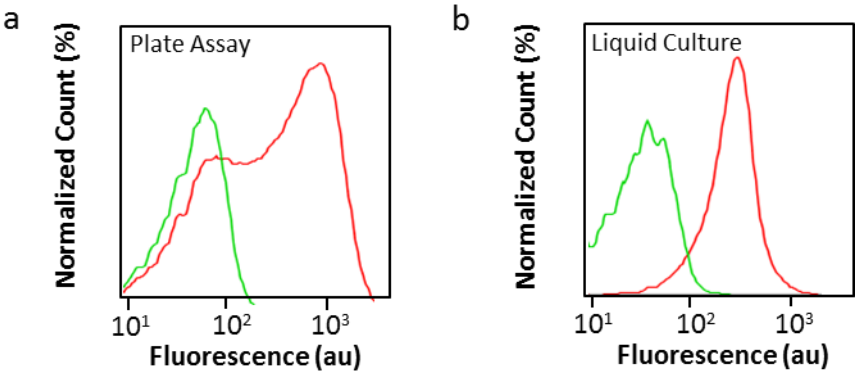

Supplementary Figure 8: Distributions generated by a NOT A gate are compared for liquid and plate cultures. a, b, Cells containing plasmid pNOR1030 and pCI-YFP were grown on an agar plate **(a)** or liquid media **(b)**. Red and green lines represent populations grown for 12 hours in media with no inducer or 10 mM arabinose, respectively.

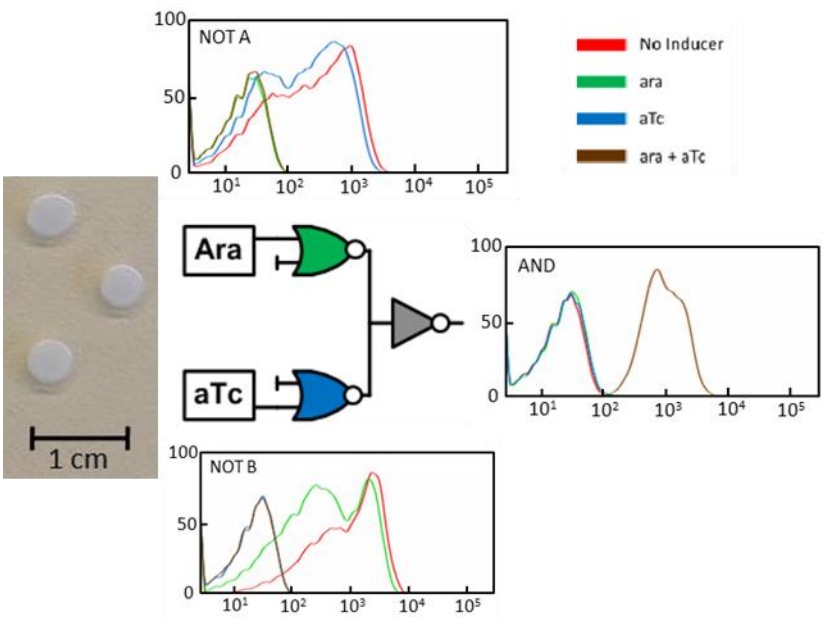

Supplementary Figure 9: The effect of population averaging is shown. The cytometry distributions of the final AND gate and its component circuits are shown. Although the intermediate colonies have broad distributions, the AND gate shows a unimodal distribution. The data for each circuit was generated independently, where YFP is the output of the last circuit (Supplementary Figure 6).

4. Robustness in Plate Assay Conditions

The robustness of the plate assay is determined with respect to the distance between sender/receiver colonies and the time and density at which they are spotted. First, to measure the distance dependence, a sender colony (1 µL of overnight culture of cells harbouring pNOR-1020 and pCI-LasI plasmids) was spotted in the middle of an agar plate. After 12 hours, the receiver colony (1 µL of washed overnight culture of cells harbouring plasmid pOR30 and pSB3K3-empty) was spotted 7 mm away (centre-to-centre) from the sender colony. The receiver colony acts as a Buffer gate with 3OC12-HSL as the input and the sender colony constitutively expresses 3OC12-HSL. After 12 hours of growth, the whole receiver cell colony is scrapped from the plate using an inoculating loop, diluted into PBS + 2 mg/mL Kan solution, and analysed using flow cytometry. As the distance between colonies increases, the fluorescence output of the receiver colony declines (Supplementary Figure 10a). At 28 mm apart, the output is reduced to basal level.

Second, the robustness was determined to the initial spotting density of the sender colony (Supplementary Figure 10b). The density was varied over two orders of magnitude. Here, 1× density is defined as spotting 1 µL of washed overnight culture of the sender colony onto an agar plate. Changing the density over this range did not affect the fluorescence output of the receiver cell significantly.

Finally, the time interval between spotting the sender and receiver colonies was varied (Supplementary Figure 10c). The spotting interval of all plate assays described previously in the main text had all been set at 12 hours. In this sender-receiver assay, reducing the time interval down to 0 hour only slightly reduced the output of the receiver cell.

A Finite Element Method model describing sender colony growth, AHL production, AHL diffusion, and YFP production in the receiver colony was developed. The growth of a colony is modelled as

$$\frac{dN_S}{dt} = k_N N_S \cdot (1 - \frac{N_S}{N_{\max}}) \quad , \tag{10}$$

$$\frac{dN_R}{dt} = k_N N_R \cdot (1 - \frac{N_R}{N_{\max}}) \quad , \tag{11}$$

where N_S (N_R) is the number of cells in the sender (receiver) colony, N_{max} is the maximum number of cells in a colony, and k_N is the growth rate of the cells. The diffusion and degradation of AHL is modelled as a reaction-diffusion equation

$$\frac{dC_A}{dt} = D_A \left[\frac{1}{r} \frac{\partial}{\partial r} r \left(\frac{\partial C_A}{\partial r} \right) \right] - \gamma_A C_A \quad , \tag{12}$$

where C_A is the concentration of AHL, D_A is the diffusion constant for AHL on a plate, and γ_A is the AHL degradation rate. It is assumed that there is no diffusion in the z axis. The distance $r = 0$ is defined as the centre of the sender colony and $r = r_R$ is the centre of the receiver colony. The production of YFP by the receiver colony is

$$\frac{dY}{dt} = \alpha_Y N_R P_{Las}(C_A) - \gamma_Y Y \quad , \tag{13}$$

where α_Y is the production rate of YFP, $P_{Las}(C_A)$ is the activity of the promoter as a function of AHL (Equation 5), γ_Y is the degradation rate of YFP, and Y is the total number of YFP in the colony (in au). The fluorescence per cell is given by Y/N_R. The boundary conditions are

$$J\big|_{r=0} = \frac{\alpha_A N_S}{2\pi r_c d_c} \quad \text{and} \quad J\big|_{r=5} = 0 \quad , \tag{14}$$

which represent the production of AHL at the sender colony and the edge of the plate (5 cm), respectively. The sender cell is treated as a point source with a rate constant α_A. This is converted to a flux by dividing by the surface area of a colony, where r_c is the radius and d_c is the depth. All of the model parameters are described in Supplementary Table 3.

One hundred discrete elements corresponding to the radially symmetric AHL concentrations (r = 0-5 cm) were used. Derivatives with respect to the radius are computed as differences between these discrete elements. These set of equations are numerically solved from time t=0 to t=24 hours using ode15s function in MATLAB with the following initial conditions: $N_S(0,0) = 10^6$ cells, $N_R(r_R,0) = 0$ cells and $A = Y = 0$. At t=12 hours (or at various interval for Supplementary Figure 10c), $N_R(r_R,12)$ is set to 10^6 cells, representing the spotting of the receiver colony. Output of the receiver colony is calculated as Y/N_R at 12 hours after the receiver colony's spotting. This model closely predicts the behaviour observed in the sender-receiver assay under the tested conditions (Supplementary Figure 10).

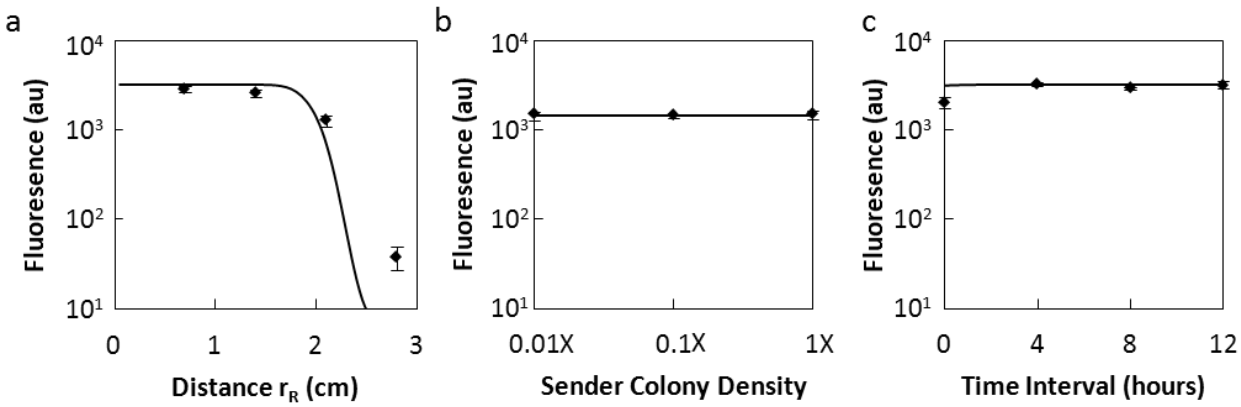

Supplementary Figure 10: Distance, time interval, and density dependence of the plate assay. The solid lines were generated using the PDE model (Equations 10-13). Fluorescence values and their error bars are calculated as averages and one standard deviation from three experiments.

Supplementary Table 3: Parameters for the PDE Model

Parameters	Description	Value	Unit	Ref
N_{max}	Maximum number of cells in a colony	3.3×10^9	cells	9
k_N	Cell growth rate	1.38	hr^{-1}	10
D_A	3OC12-HSL diffusion constant	6×10^{-3}	$cm^2\ hr^{-1}$	11 a
α_A	3OC12-HSL production rate	1.6×10^{-8}	nmoles hr^{-1} $cell^{-1}$	12 b
α_Y	YFP production rate	100	au hr^{-1} $cell^{-1}$	
γ_A	3OC12-HSL degradation rate	0.012	hr^{-1}	13
γ_Y	YFP degradation rate	0.0289	hr^{-1}	14
r_c	Radius of colony	0.2	cm	
d_c	Depth of colony	0.1	cm	

[a] This value is higher than previously described.
[b] Value estimated based the RhlI k_{cat} = 960 AHL molecules per hour and using an estimated value of 10^4 proteins per cell. This produces a rate of 2666 AHL molecules per second per cell, which is consistent with published values[15].

The effect of different timing delays was also determined for a multi-layered circuit (the XOR gate) (Supplementary Figure 11). Longer delays ensure that sufficient signalling molecules have been produced such that proper signal propagation can occur for each layer. Reducing the interval from 12 to 6 hours produces an equivalent XOR behaviour. However, when all four XOR colonies were spotted at the same time (0 hours), the quality of the logic function is reduced significantly.

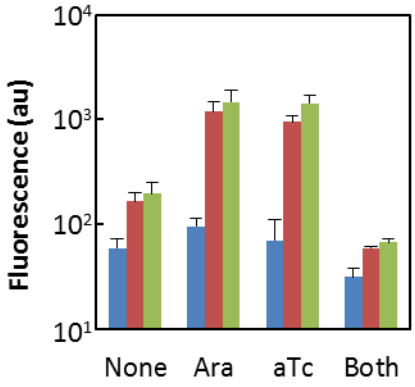

Supplementary Figure 11: The dependence of the XOR gate on the time delay between spotting colonies. The time interval of colony spotting between layers was: 0 hrs (blue), 6 hrs (red), and 12 hours (green). The fluorescence of the last colony (Cell 4) was measured 12 hours after the spotting of the last layer by flow cytometry. Fluorescence values and their error bars are calculated as averages and one standard deviation from three experiments.

5. Liquid Culture Assay

Experiments were performed to determine how the multi-strain circuits perform when mixed together in liquid culture. The four strains that make up the XOR circuit (Fig. 3) were chosen as the test case. For all of the liquid culture experiments, the strains had to be maintained in the OFF state before they were mixed together at *t*=0. If the strains were not maintained in the OFF state, they transiently produce AHL (or YFP) before the complete circuit can reach steady-state. These transient errors result in permanent failures in the complete circuit. In the case of the XOR circuit, the proper logic is not recovered (not shown). This is related to faults that can occur in asynchronous computing. In all of the following experiments, the strains were maintained in the OFF state prior to their participation in the circuit.

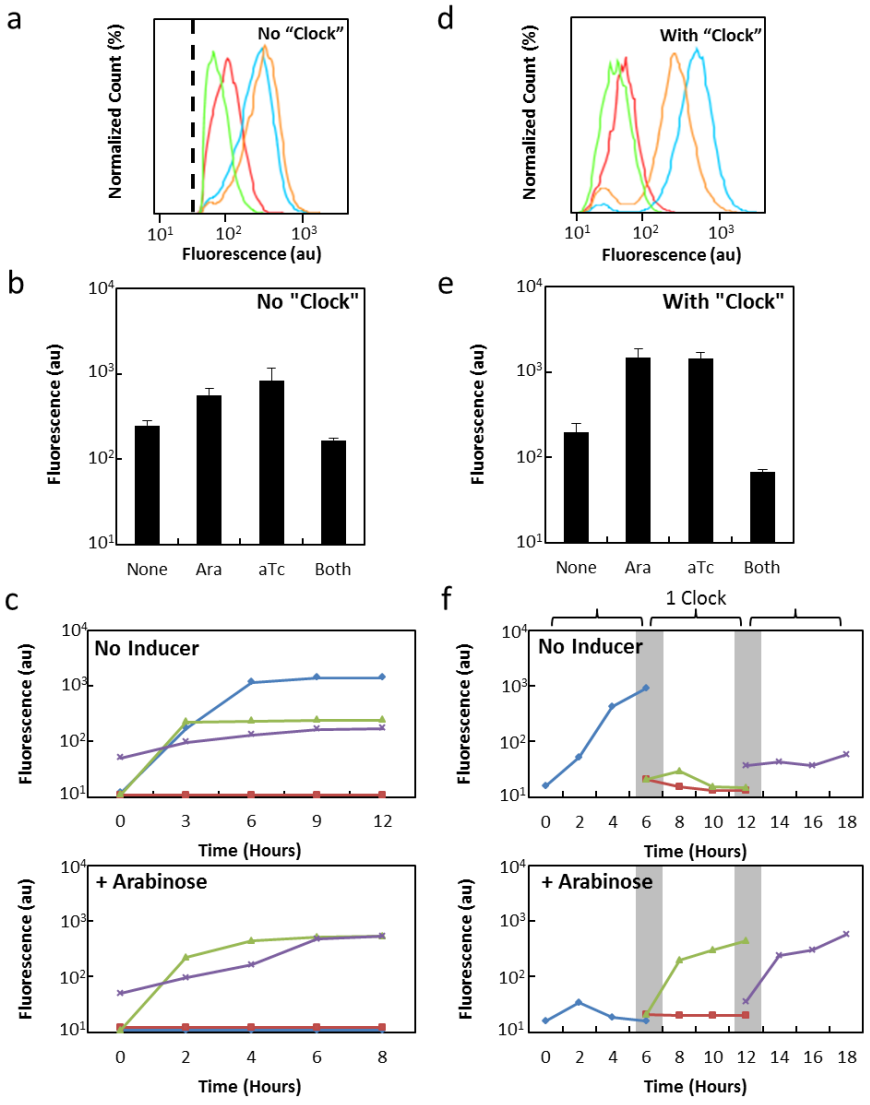

Supplementary Figure 12: The XOR circuit as measured in liquid culture. XOR logic computation was performed in liquid culture with (A-C) and without (D-F) an external clock. **a, d,** Representative cytometry histograms of the output strain (Cell 4) at the end of the assay. The four input states are when media is supplemented with no inducer (red), 10 mM Ara (blue), 50 ng/mL aTc (orange), or both inducers (green). In the co-culture when all cells are grown simultaneously **(a)**, the white cells have to be subtracted from the distribution to visualize the data for the YFP-producing strain in the last layer. This subtraction threshold is shown by the dashed line. **b, e,** The average florescence for each combination of inducers is shown. Fluorescence values and their error bars are calculated as averages and one standard deviation from three experiments. **c, f,** A complete timecourse is shown for a representative combination of inducers for an OFF (top) and ON (bottom) output. The fluorescence output of Cell 1 (blue), Cell 2 (red), Cell 3 (green), and Cell 4 (purple) are shown for no inducer and 10 mM arabinose. The grey bars in **(f)** represent artificial "clock" events in which the supernatant of a culture was collected and then used to grow cells of the next logic layer.

Two types of liquid cultures were performed. In the first, all of the strains are inoculated together at *t*=0 and grown as a co-culture. In the second, the strains associated with each layer are inoculated, grown, and then removed from the culture before the next layer is seeded. In effect, this implements an external "clock" on the system, where each layer is allowed sufficient time to complete before the next layer is initiated. We refer to these experiments as "no clock" and "clock," respectively. The detailed methods appear at the end of this section.

When there is no clock, the bacterial populations produced XOR logic although there is only a 2-fold change between the ON and OFF states (Supplementary Figure 12a-c). This is likely due to inability of Cell 1 to quickly accumulate AHL to a detectable level, while Cells 2-4 are growing and performing their respective logic operations. This can be seen in the timecourse, where in the absence of inducer, Cells 3 do not turn OFF because of the absence of AHL produced by Cell 1. This creates faulty output production in downstream logic gates, which degrades the signal of the complete XOR circuit.

The plate assays have an effective external clock when the colonies associated with each layer are spotted after 12 hour delays. This is replicated in liquid culture by growing cells of the first layer for 6 hours, pelleting down the cells, collecting the supernatant, and using it for culture of subsequent layers. This is repeated until the last layer of the circuit is grown. This yields an improved XOR function, with a 6-fold change between the ON and OFF states, which is nearly the same as that observed in the plate assay (Supplementary Figure 12d-f). In the timecourses, all of the cells generated the correct behaviour at all times.

No "clock" liquid culture method: Independent overnight cultures of the four strains that make up the XOR logic circuit (Fig. 3) were grown in liquid LB media supplemented with 10 mM Ara and 50 ng/mL aTc in order to keep them in the OFF state for 18 hours. These overnight cultures were washed twice (two minutes-5,000 r.p.m. centrifugation, decanting, followed by resuspension into the same volume) to remove arabinose and aTc within the media. The washed cultures were used to seed 2 mL of fresh liquid LB culture (1:50 dilution) supplemented with no inducer, 10 mM Ara, 50 ng/mL aTc, or 10 mM Ara and 50 ng/mL aTc in a culture tube. After twelve hours of growth (37ºC, 250 r.p.m. shaking), the cultures were analysed for YFP expression using flow cytometry. Note that to make the XOR logic circuit, four cell populations were seeded into the culture. However, only Cell 4 expresses YFP. Thus, in the flow cytometry data, approximately three quarters of the cells will exhibit no YFP fluorescence. The population distribution of this assay showed two separable peaks that correspond to the white cells and Cell 4 populations. These white cells were gated out so that only fluorescence value of Cell 4 was reported as the output of the XOR circuit.

With "clock" liquid culture method: In this assay, the overnight cultures of the bacterial strains were prepared as before. The washed culture of Cell 1 was seeded in 2 mL of fresh liquid LB (1:50 dilution) supplemented with no inducer, 10 mM Ara, 50 ng/mL aTc, or 10 mM Ara and 50 ng/mL aTc. After six hours of growth (37ºC, 250 r.p.m. shaking), these cultures were filtered (0.22 μm) to remove cells from the culture supernatant. 1 mL of fresh LB media (supplemented with the appropriate inducers) was added to 1 mL of the filtered supernatant to give fresh nutrients for the subsequent culture. Cells from the second layer (ie. Cell 2 and Cell 3) were then seeded (1:50 dilution) unto the diluted supernatant. After six hours (37ºC, 250 r.p.m. shaking), the same filtration and supernatant dilution was performed and Cell 4 was seeded (1:50 dilution). After another six hours (37ºC, 250 r.p.m. shaking), sample of the culture was taken for flow cytometry assay.

Timecourse assay method: Timecourses were performed by taking cell aliquots from the liquid culture and assaying them for YFP production. The outputs of Cell 1, Cell 2, and Cell 3 were measured by replacing the output plasmid of these cells with YFP reporter plasmid (pCI-YFP) in a repeat experiment.

The "no clock" culture contains mixed populations of the four cell populations. Cytometry distributions of this mixed cultures for all timepoints showed either a single peak undistinguishable to that of the white cells population or two separable peaks that correspond to the white cell and fluorescent cell populations. In the first case, we set the fluorescence value for those populations to be at "white" cells background level. For the second case, the white cells were gated out.

6. Strains, Plasmid Maps, and Plasmid Constructions

Plasmid pOR10, pOR20, pOR30, pOR1020, pOR1030, pOR2030, pOR2010, pNOR1020, pNOR1030, pNOR2030, and pNOR40 use BBa_J64100 (www.partsregistry.org) as their backbone. Plasmid pCI-YFP, pCI-LasI, and pCI-RhlI use pSB3K3[16] as their backbone. ReceiverA-YFP plasmid is a derivative of plasmid pFNK-202-qsc119 obtained from previous study[17] with the original GFP reporter replaced with YFP. All of the promoters and genes associated with quorum sensing components were obtained from *Pseudomonas aeruginosa* genomic DNA (ATCC #47085D-5)[18].

For Fig. 1c, cells harbouring plasmid pOR10 or pOR20 were used to characterize the transfer function of single promoter P_{BAD} and P_{Tet} respectively. Cells with plasmid pOR1020 were used for the P_{BAD}-P_{Tet} OR gate characterization. Cells with plasmid pNOR1020 and pCI-YFP were used for the P_{BAD}-P_{Tet} NOR gate characterization. For Fig. 2, cells with plasmid pOR1020, pOR1030, or pOR2030 were used to characterize the transfer function of P_{BAD}-P_{Tet}, P_{BAD}-$P_{Las,}$ or P_{Tet}-P_{Las} OR Gate respectively. Cells with plasmid pCI-YFP and one of the following plasmid: pNOR1020, pNOR1030, or pNOR2030, were used for the P_{BAD}-P_{Tet}, P_{BAD}-$P_{Las,}$ or P_{Tet}-P_{Las} NOR gate characterization respectively. For Fig. 3 and Fig. 4, refer to Supplementary Table 5 for plasmid composition of each colour coded bacterial strain.

Supplementary Table 4: List of parts used in this study

Part Name	Description and Source
P_{BAD}	araBAD promoter (-284 to +20 nt from transcription start site)[19]
P_{Tet}	PLtetO-1 promoter (-54 to +0 nt from transcription start site)[20] with two base pairs changes: G43T and C47A
P_{Las}	RsaL promoter (-76 to -18 nt from RsaL start codon)[18]
P_{Rhl}	RhlA promoter (-63 to +10 nt from transcription start site)[18]
P_{CI}	P_R promoter from lambda bacteriophage (-49 to +0 nt from transcription start site)[21]
YFP	Enhanced Yellow Fluorescent Protein[22]
CI	Lambda CI repressor (BBa_C0051)[21]
Constitutive Promoter	Synthetic σ70 constitutive promoter (BBa_J23117, DNA sequence: ttgacagctagctcagtcctagggattgtgctagc)
Terminator	Double terminator (T1 from *E. coli* rrnB and TE from coliphage T7, DNA sequence: ccaggcatcaaataaaacgaaaggctcagtcgaaagactgggcctttcgttttatctgttgtttgtcggtgaacgctctctactagagtcacactggctcaccttcgggtgggcctttctgcgttta)
LasI	LasI coding sequence[18]
RhlI	RhlI coding sequence[18]
AraC	AraC coding sequence[19]
TetR	TetR coding sequence[20]
LasR	LasR coding sequence[18]
RhlR	RhlR coding sequence[18]

Supplementary Table 5: List of strains used in this study[a]

Colour Code[b]	Logic Gate	Input Promoters	Output Gene	Plasmids
Grey	NOT	P_{Rhl}	YFP	pNOR40, pCI-YFP
Brown	Buffer	P_{Rhl}	YFP	ReceiverA-YFP[d], pVJ64100-empty
Purple	OR	P_{BAD}-P_{Tet}	YFP	pOR1020
Orange	OR	P_{BAD}-P_{Las}	YFP	pOR1030
Yellow	OR	P_{Tet}-P_{Las}	YFP	pOR2030
Red[c]	NOR	P_{BAD}-P_{Tet}	YFP	pNOR1020, pCI-YFP
Red[c]	NOR	P_{BAD}-P_{Tet}	LasI	pNOR1020, pCI-LasI
Green[c]	NOR	P_{BAD}-P_{Las}	YFP	pNOR1030, pCI-YFP
Green[c]	NOR	P_{BAD}-P_{Las}	RhlI	pNOR1030, pCI-RhlI
Blue[c]	NOR	P_{Tet}-P_{Las}	YFP	pNOR2030, pCI-YFP
Blue[c]	NOR	P_{Tet}-P_{Las}	RhlI	pNOR2030, pCI-RhlI

[a] All strains are based on *E. coli* DH10B.
[b] Colour coding corresponds to the colours shown in Fig. 3 and Fig. 4 in the main text.
[c] Two versions of these gates are produced. When the gate is the last in a circuit, then its output is YFP. If it connects to another layer, the output is an enzyme that produces a quorum signal.
[d] ReceiverA-YFP plasmid is a derivative of plasmid pFNK-202-qsc119 obtained from previous study[17] with the original GFP reporter exchanged with YFP.

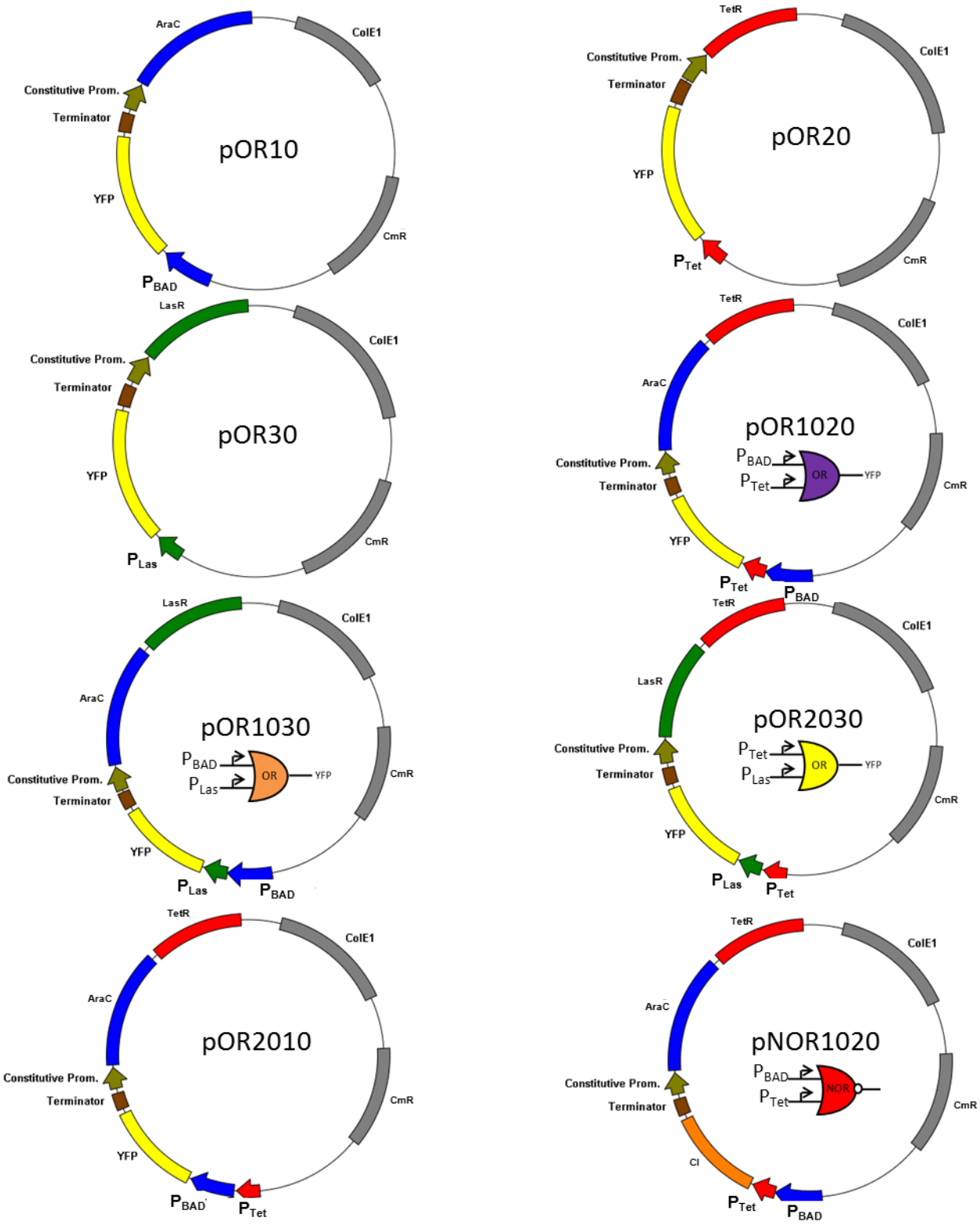
pOR10
AraC
ColE1
Constitutive Prom.
Terminator
YFP
CmR
P BAD
pOR20
TetR
ColE1
Constitutive Prom.
Terminator
YFP
P Tet
CmR
pOR30
LasR
ColE1
Constitutive Prom.
Terminator
YFP
CmR
P Las
pOR1020
TetR
ColE1
AraC
P BAD
P Tet
OR
YFP
Constitutive Prom.
Terminator
CmR
YFP
P Tet
P BAD
pOR1030
LasR
ColE1
AraC
P BAD
P Las
OR
YFP
Constitutive Prom.
Terminator
CmR
YFP
P Las
P BAD
pOR2030
TetR
ColE1
LasR
P Tet
P Las
OR
YFP
Constitutive Prom.
Terminator
CmR
YFP
P Las
P Tet
pOR2010
TetR
ColE1
AraC
Constitutive Prom.
Terminator
CmR
YFP
P BAD
P Tet
pNOR1020
TetR
ColE1
AraC
P BAD
P Tet
NOR
Constitutive Prom.
Terminator
CmR
CI
P Tet
P BAD

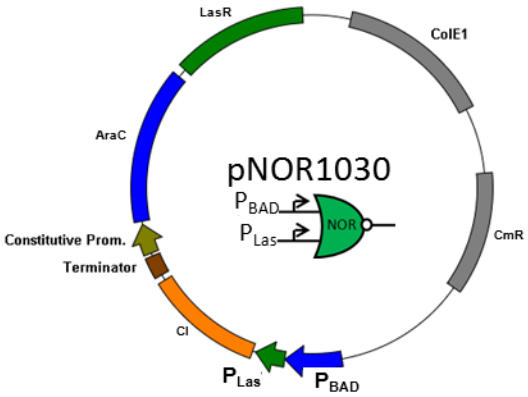
LasR
ColE1
AraC
pNOR1030
P BAD
P Las
NOR
Constitutive Prom.
Terminator
CmR
CI
P Las
P BAD

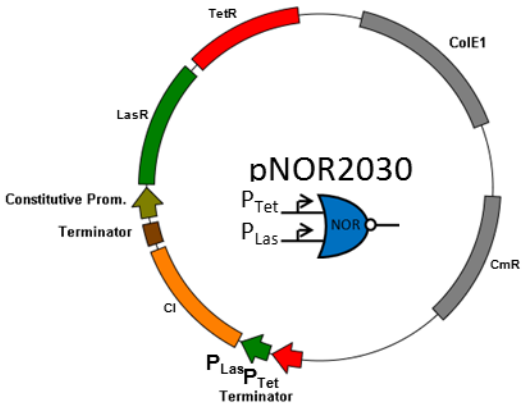
TetR
ColE1
LasR
pNOR2030
P Tet
P Las
NOR
Constitutive Prom.
Terminator
CmR
CI
P Las
P Tet
Terminator

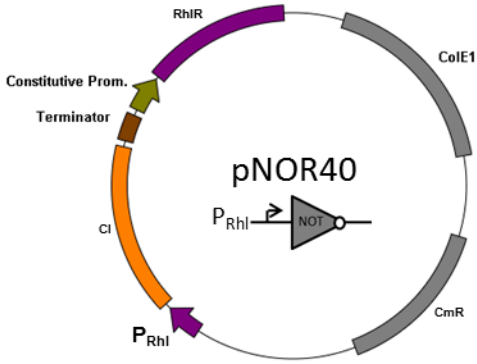
RhlR
ColE1
Constitutive Prom.
Terminator
pNOR40
P RhlI
NOT
CI
CmR
P RhlI

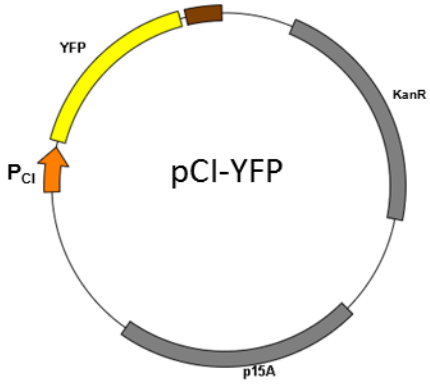
YFP
KanR
P CI
pCI-YFP
p15A

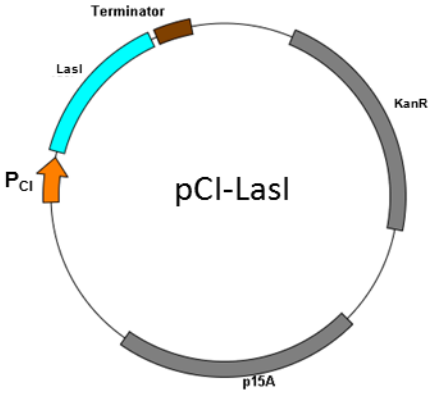
Terminator
LasI
KanR
P CI
pCI-LasI
p15A

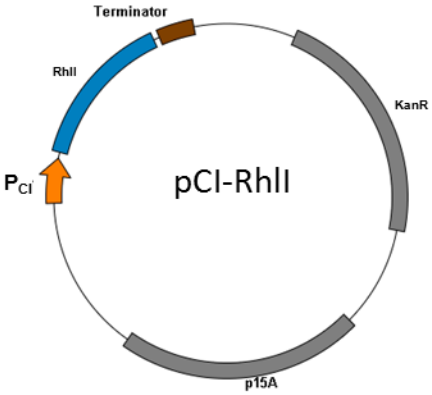
Terminator
RhlI
KanR
P CI
pCI-RhlI
p15A

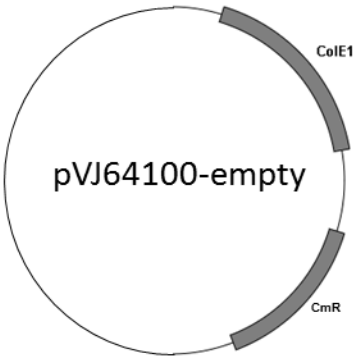
ColE1
pVJ64100-empty
CmR

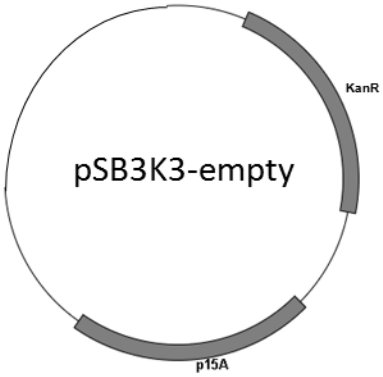
KanR
pSB3K3-empty
p15A

7. Supplemental References

1. Ackers, G. K., Johnson, A. D. & Shea, M. A. Quantitative model for gene regulation by lambda phage repressor. *Proc Natl Acad Sci U S A* **79**, 1129-1133, (1982).
2. Bintu, L. *et al.* Transcriptional regulation by the numbers: applications. *Curr Opin Genet Dev* **15**, 125-135, (2005).
3. Bintu, L. *et al.* Transcriptional regulation by the numbers: models. *Curr Opin Genet Dev* **15**, 116-124, (2005).
4. Passador, L. *et al.* Functional analysis of the Pseudomonas aeruginosa autoinducer PAI. *J Bacteriol* **178**, 5995-6000, (1996).
5. Anderson, J. C., Voigt, C. A. & Arkin, A. P. Environmental signal integration by a modular AND gate. *Mol Syst Biol* **3**, 133, (2007).
6. Grigorova, I. L., Phleger, N. J., Mutalik, V. K. & Gross, C. A. Insights into transcriptional regulation and sigma competition from an equilibrium model of RNA polymerase binding to DNA. *Proc Natl Acad Sci U S A* **103**, 5332-5337, (2006).
7. Tabor, J. J. *et al.* A synthetic genetic edge detection program. *Cell* **137**, 1272-1281, (2009).
8. Yokobayashi, Y., Weiss, R. & Arnold, F. H. Directed evolution of a genetic circuit. *Proc Natl Acad Sci U S A* **99**, 16587-16591, (2002).
9. Mashimo, K., Nagata, Y., Kawata, M., Iwasaki, H. & Yamamoto, K. Role of the RuvAB protein in avoiding spontaneous formation of deletion mutations in the Escherichia coli K-12 endogenous tonB gene. *Biochem Biophys Res Commun* **323**, 197-203, (2004).
10. Bernstein, J. A., Khodursky, A. B., Lin, P. H., Lin-Chao, S. & Cohen, S. N. Global analysis of mRNA decay and abundance in Escherichia coli at single-gene resolution using two-color fluorescent DNA microarrays. *Proc Natl Acad Sci U S A* **99**, 9697-9702, (2002).
11. Basu, S., Gerchman, Y., Collins, C. H., Arnold, F. H. & Weiss, R. A synthetic multicellular system for programmed pattern formation. *Nature* **434**, 1130-1134, (2005).
12. Parsek, M. R., Val, D. L., Hanzelka, B. L., Cronan, J. E., Jr. & Greenberg, E. P. Acyl homoserine-lactone quorum-sensing signal generation. *Proc Natl Acad Sci U S A* **96**, 4360-4365, (1999).
13. Flagan, S., Ching, W. K. & Leadbetter, J. R. Arthrobacter strain VAI-A utilizes acyl-homoserine lactone inactivation products and stimulates quorum signal biodegradation by Variovorax paradoxus. *Appl Environ Microbiol* **69**, 909-916, (2003).
14. Andersen, J. B. *et al.* New unstable variants of green fluorescent protein for studies of transient gene expression in bacteria. *Appl Environ Microbiol* **64**, 2240-2246, (1998).
15. Alberghini, S. *et al.* Consequences of relative cellular positioning on quorum sensing and bacterial cell-to-cell communication. *FEMS Microbiol Lett* **292**, 149-161, (2009).
16. Shetty, R. P., Endy, D. & Knight, T. F., Jr. Engineering BioBrick vectors from BioBrick parts. *J Biol Eng* **2**, 5, (2008).
17. Brenner, K., Karig, D. K., Weiss, R. & Arnold, F. H. Engineered bidirectional communication mediates a consensus in a microbial biofilm consortium. *Proc Natl Acad Sci U S A* **104**, 17300-17304, (2007).
18. Pesci, E. C., Pearson, J. P., Seed, P. C. & Iglewski, B. H. Regulation of las and rhl quorum sensing in Pseudomonas aeruginosa. *J Bacteriol* **179**, 3127-3132, (1997).
19. Lee, N. L., Gielow, W. O. & Wallace, R. G. Mechanism of araC autoregulation and the domains of two overlapping promoters, Pc and PBAD, in the L-arabinose regulatory region of Escherichia coli. *Proc Natl Acad Sci U S A* **78**, 752-756, (1981).
20. Lutz, R. & Bujard, H. Independent and tight regulation of transcriptional units in Escherichia coli via the LacR/O, the TetR/O and AraC/I1-I2 regulatory elements. *Nucleic Acids Res* **25**, 1203-1210, (1997).
21. Stayrook, S., Jaru-Ampornpan, P., Ni, J., Hochschild, A. & Lewis, M. Crystal structure of the lambda repressor and a model for pairwise cooperative operator binding. *Nature* **452**, 1022-1025, (2008).
22. Cormack, B. P., Valdivia, R. H. & Falkow, S. FACS-optimized mutants of the green fluorescent protein (GFP). *Gene* **173**, 33-38, (1996).